Chandra follow-up of unidentified sources in the *INTEGRAL*/IBIS 1000-orbit catalogue

F. Ursini, L. Bassani

INAF-OAS Bologna, Area della Ricerca del CNR

Report n. OAS/1/2018
July 2018

Table 1: Unidentified sources from the 4th *INTEGRAL* catalogue. The *Chandra* Obs. Id. is given in the last column.

RA	DEC	name	Obs. Id.
03:59:53.5	50:43:40.8	IGR J03599+5043	18971
15:03:45.8	-60:21:25.2	IGR J15038-6021	18970
15:54:06.5	-56:12:57.6	IGR J15541-5613	18972
16:11:53.8	-35:45:14.4	IGR J16120-3543	18983
16:18:08.0	-54:06:09.8	IGR J16181-5407	18975
16:24:21.8	-45:55:22.8	IGR J16246-4556	18974
16:48:34.8	-30:01:08.4	IGR J16482-2959	18982
17:50:53.0	-32:19:48.0	IGR J17508-3219	18976
17:09:43.7	-25:28:12.0	IGR J17096-2527	18980
17:11:50.2	-31:55:37.2	IGR J17118-3155	18977
19:29:29.8	13:27:05.4	IGR J19294+1327	18973
20:30:55.3	38:33:39.4	IGR J20310+3835	18969
20:41:32.2	32:13:08.4	IGR J20413+3210	18978

1 Introduction

We report on *Chandra* observations of so far unidentified *INTEGRAL*/IBIS sources, in the Galactic plane, listed in the cat1000 catalogue (Bird et al., 2016). Since the IBIS coordinate error box is generally of a few arcmin, high-resolution *Chandra* observations were obtained (PI: Tomsick) to allow for the identification of counterparts and constrain the soft X-ray spectrum. Up to the end of June 2018, 15 sources have been observed by *Chandra*, with an exposure of 5 ks each. We discuss the 12 observations whose data are public as of the end of June 2018. The basic data of the sources are reported in Table 1.

2 The sources

The *Chandra* data were reduced with the package CIAO v4.10 and reprocessed with the standard tool CHANDRA_REPRO. We inspected the *Chandra* images both visually and with the detection tool WAVDETECT, an algorithm used to identify source candidates within a single observation (Freeman et al., 2002). We select a significance threshold parameter of 10^{-6}, which corresponds to one possibly spurious pixel in one CCD (1024×1024 pixels). We also require the source flux to be significant at ≥ 3-σ level, that typically correspond to ~ 10 net source counts on-axis and $\sim 20-30$ net counts off-axis (Evans et al., 2010). The typical *Chandra* upper limit to the 0.4–6 keV flux from a 5-ks exposure is 6×10^{-13} ergs s^{-1} cm^{-2}. The typical position uncertainty is of a few arcsec.

2.1 IGR J03599+5043

Detected by IBIS in a 2303.8 day outburst from MJD=52816.5.
No source is detected in the *Chandra* image.

2.2 IGR J15038-6021

Detected as a persistent source in the 18-60 keV band.
Two sources are detected in *Chandra*, both within the 90% error box of IBIS (Fig. 1). Source #1 has 290 counts (190 counts above 3 keV), while source #2 has only 40 counts (18 above 3 keV). We thus identify IGR J15038-6021 with source #1. This source was also detected in XRT and might have two optical and one IR counterparts (Landi et al., 2017).
Chandra coordinates:
RA = 15:04:15.74
DEC = -60:21:23.02
error box = 2.5 arcsec
The *Chandra* spectrum is plotted in Fig. 2, with the best-fitting power law. The spectrum is flat, with photon index $\Gamma = 0.0 \pm 0.2$. The 0.3–10 keV flux is 3×10^{-12} ergs s^{-1} cm^{-2}.
The small *Chandra* error box allows us to pinpoint a single optical counterpart and exclude the IR association suggested in Landi et al. (2017).

2.3 IGR J15541-5613

Detected in a 949.5 day outburst from MJD=52651.2.
One weak source is detected in *Chandra* within the 90% error box of IBIS (Fig. 3). The source has only 42 counts (24 above 3 keV).
Chandra coordinates:
RA = 15:54:13.07
DEC = -56:09:32.39
error box = 2 arcsec
The 0.3–10 keV flux is 4×10^{-13} ergs s^{-1} cm^{-2}.

2.4 IGR J16120-3543

Detected in a 127.3 day outburt from MJD=52911.9.
Only a very weak source is detected, having 17 total counts (9 above 3 keV).

2.5 IGR J16181-5407

Detected as a persistent source in the 18-60 keV band.
One source is detected, close to the nominal IBIS coordinates (Fig. 4), and having 276 counts (237 above 3 keV).
Chandra coordinates:
RA = 16:18:07.73
DEC = -54:06:12.14
error box = 2 arcsec
The *Chandra* spectrum (Fig. 2) is flat, with photon index $\Gamma = -0.3 \pm 0.3$. There is a hint for the presence of photoelectric absorption with $N_{\rm H} \sim 10^{23}$ cm^{-2} ($\Gamma \sim 1.4$ in this case), but with large uncertainties. The 0.3–10 keV flux is 3×10^{-12} ergs s^{-1} cm^{-2}.
This source has also been reported in ATel #4233 (Landi et al. 2012). It has also been repeatedly observed by XRT over the period 2011–2013, with a total significance of 14.2 σ (0.3–10 keV) of which 13.2 σ above 3 keV (Landi et al., INAF/IASF-BO n. 655/2015). The combined XRT spectrum is well described by an absorbed power law

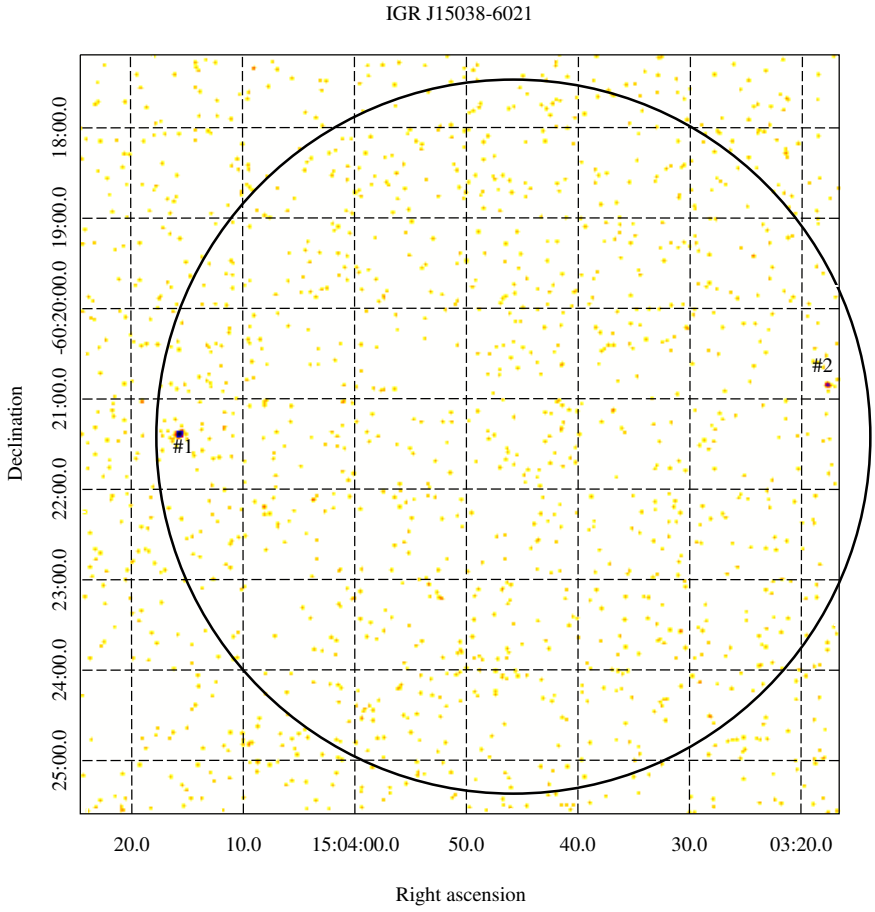

Figure 1: 3–10 keV *Chandra* image of the IGR J15038-6021 field. Source #1 is dominant.

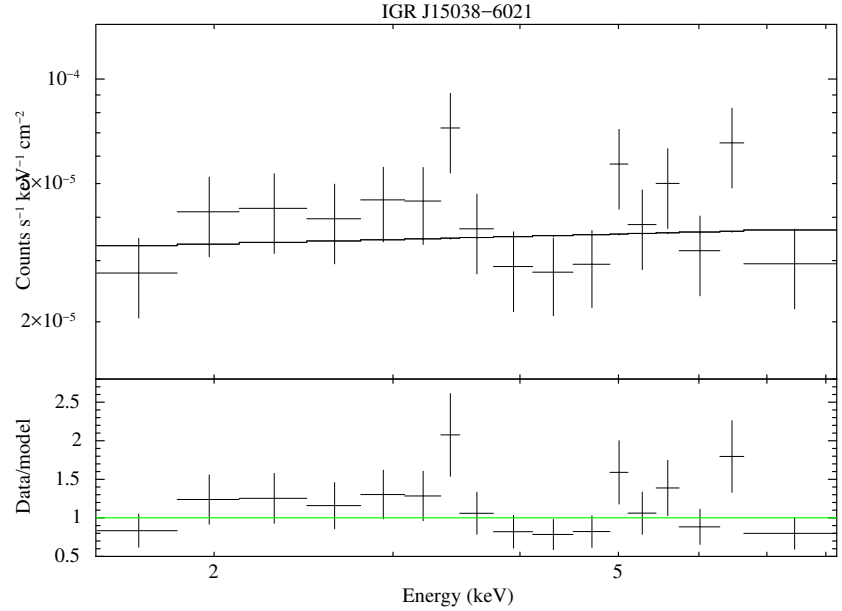

Figure 2: *Chandra* spectrum of IGR J15038-6021 (source #1).

($N_{\rm H} = 7.1\times10^{22}$ cm^{-2}, $\Gamma \simeq 1.59$ and 2–10 keV flux of 3.9×10^{-12} ergs s^{-1} cm^{-2}). This X-ray source is the optical/IR object USNO-B1.0 0358-0591923/2MASSJ 16180771-5406122, also listed in the ALL-WISE catalogue as J161807.75-540612.3 with colours W1-W2=1.176 and W2-W3=2.566, i.e. typical of AGNs (Secrest et al., 2015), suggesting that this is an absorbed AGN.

This source was also observed by *NuSTAR* on 2017-01-29 (Obs. Id. 30161006002), with a net exposure time of 59 ks, as part of the Galactic Legacy Survey (note that the *Chandra* observation was performed 4 months after, on 2017-05-20). The *NuSTAR* spectrum has a signal-to-noise ratio of 75 in the 3–30 keV band, and is typical of an absorbed AGN. A fit of the *NuSTAR* spectrum with a simple power law yields χ^2/dof = 299/172, with a clear turnover at low energies. The fit is greatly improved by including photoelectric absorption (χ^2/dof = 192/171, $\Delta\chi^2/\Delta$dof = $-107/-1$). Some positive residuals around 6 keV suggest the presence of a Fe Kα emission line. Indeed, adding a narrow Gaussian line improves the fit (χ^2/dof = 177/169, $\Delta\chi^2/\Delta$dof = $-15/-2$; the probability of chance improvement is 0.001 from an F-test). The equivalent width of the line is 100 ± 50 eV, and its energy (observer's frame) is 5.85 ± 0.15 keV. If interpreted as the neutral Fe Kα line at 6.4 keV, it would indicate a redshift of 0.085 ± 0.015. Finally, we measure a photon index $\Gamma = 1.69 \pm 0.08$ and an absorbing column density of $(8 \pm 2)\times10^{22}$ cm^{-2}. The extrapolated 0.3–10 keV flux is 4×10^{-12} ergs s^{-1} cm^{-2}, while the extrapolated 20–100 keV flux is 1.2×10^{-11} ergs s^{-1} cm^{-2} (a factor of 1.5 larger than the IBIS flux, Bird et al., 2016).

Fitting jointly the *Chandra* and *NuSTAR* spectra yields a good fit with $\chi^2 = 198/184$; the cross-calibration constant *Chandra*/*NuSTAR* is 0.49 ± 0.06 (possibly due to source variability), $\Gamma = 1.74 \pm 0.06$ and the column density is $(10 \pm 2)\times10^{22}$ cm^{-2}.

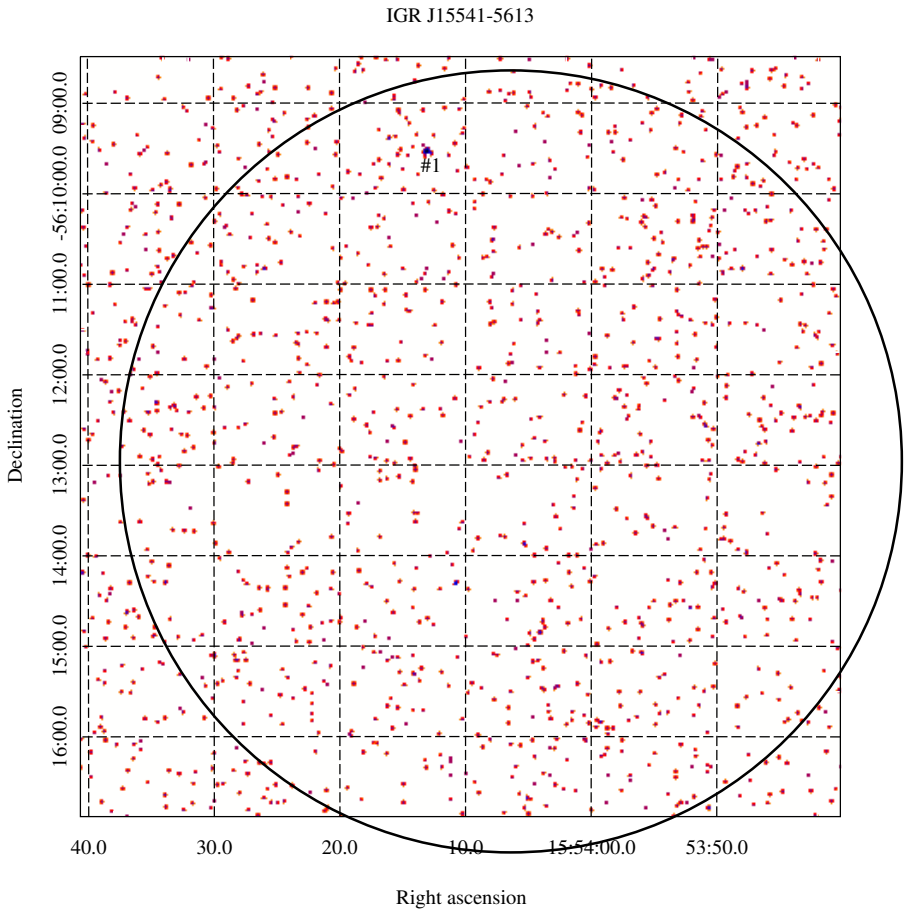

Figure 3: 3–10 keV *Chandra* image of the IGR J15541-5613 field. Only one weak source is present.

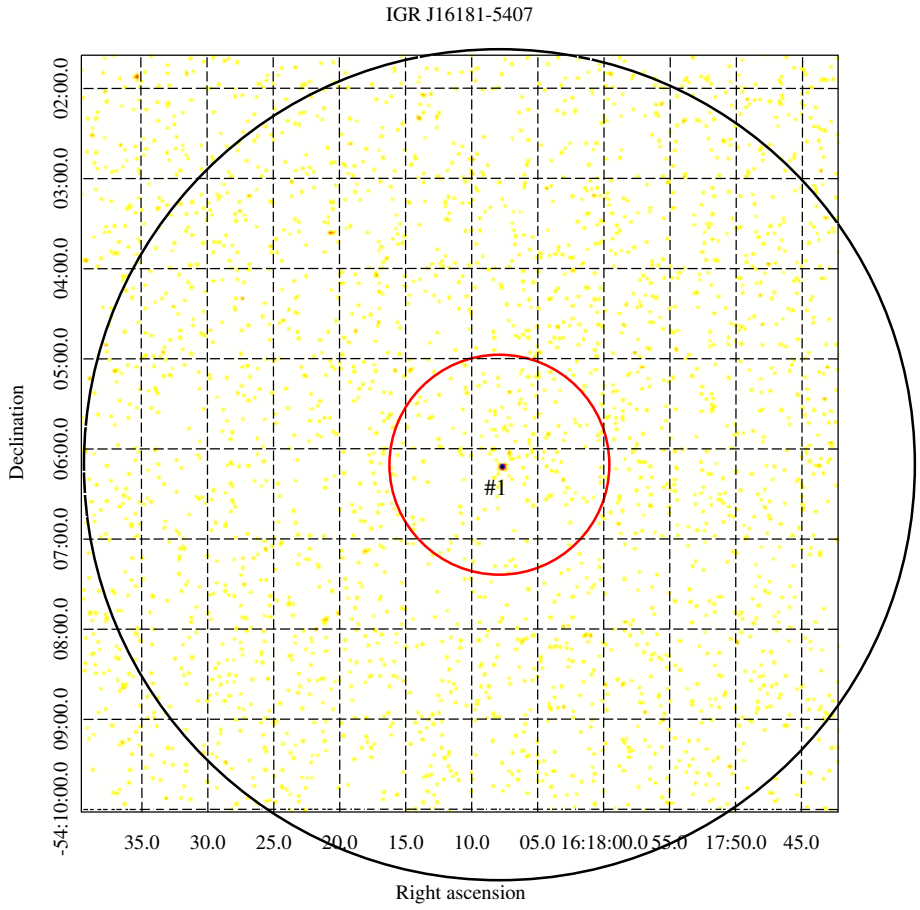

Figure 4: 3–10 keV *Chandra* image of the IGR J16181-5407 field. One source is detected. The red circle corresponds to the *NuSTAR* error box.

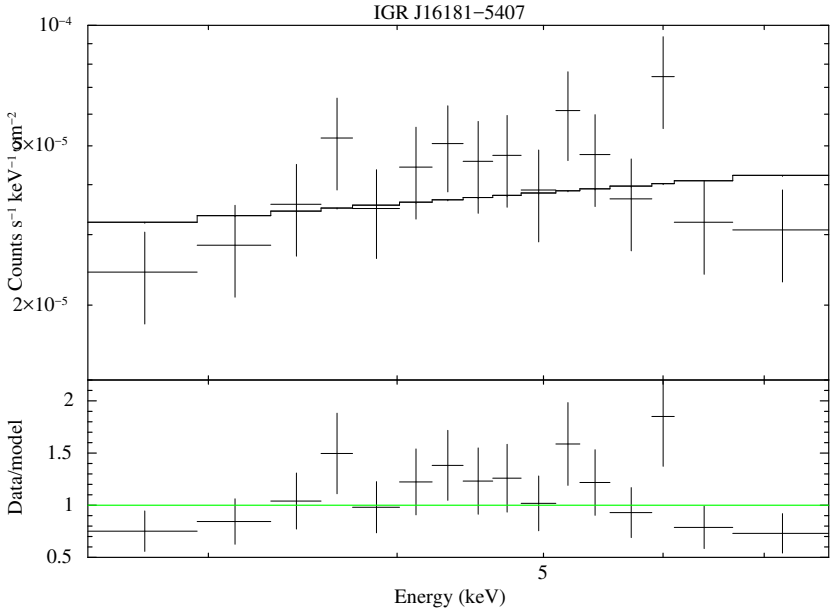

Figure 5: *Chandra* spectrum of IGR J16181-5407.

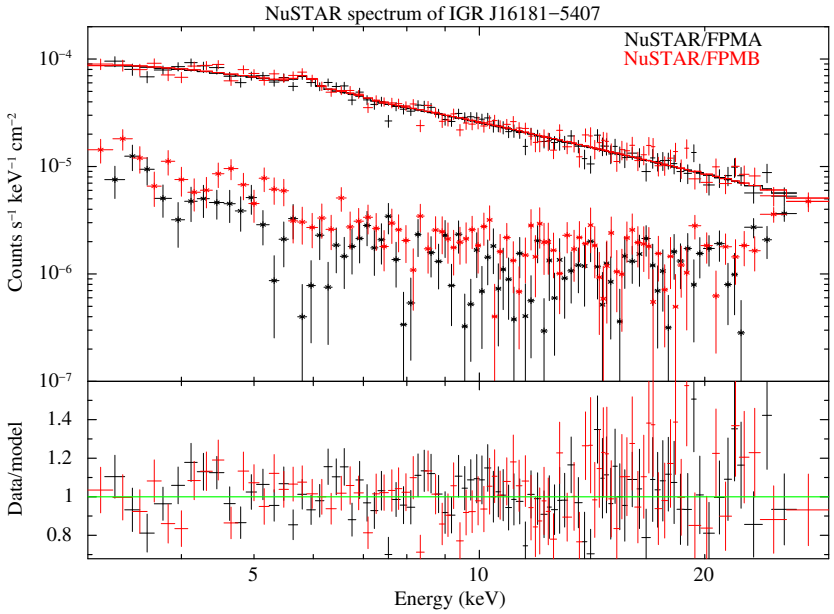

Figure 6: *NuSTAR* spectrum of IGR J16181-5407 fitted with an absorbed power law plus a narrow Gaussian line. The background is shown in the top panel.

2.6 IGR J16246-4556

Detected in a 1969.2 day outburst from MJD=53044.7.
One source is detected in *Chandra* (Fig. 7), with 133 counts (79 above 3 keV).
Chandra coordinates:
RA = 16:24:30.79
DEC = -45:55:14.06
error box = 2 arcsec
The spectrum (Fig. 8) has photon index $\Gamma = 1.0 \pm 0.4$, and the 0.3–10 keV flux is 8×10^{-13} ergs s^{-1} cm^{-2}.
This X-ray source has a unique counterpart (2MASS J16243080-4555144/ALL-WISE J162430.7-455514.2). The WISE colours of this source are W1-W2=0.176 and W2-W3=1.78, which are not typical of AGNs (Secrest et al., 2015), unless this is a heavily absorbed or Compton-thick source (Gandhi et al., 2015). A follow-up with optical spectroscopy is needed to classify this source. Note however that the source is reported in the blind HI survey of the extragalactic sky behind the Southern Milky Way (Staveley-Smith et al., 2016).

2.7 IGR J16842-2959

Detected in a 263.9 day outburst from MJD=54344.1.
No source is detected in *Chandra*.

2.8 IGR J17508-3219

Detected as a persistent source in the 18-60 keV band.
Two sources are detected in *Chandra*. One of them (#1, the brighter) is found within the 99% error box of IBIS, while the other (#2) is borderline (Fig. 9). In XRT, Landi et al. (2017) found another source within the 90% error box of IBIS, that is not detected in *Chandra*. Given the *Chandra* sensitivity and exposure time of 5 ks, we can place an upper limit to the flux of such source of 6×10^{-15} ergs s^{-1} cm^{-2} in the 0.4–6 keV band. From XRT data, the 0.4–6 keV flux was 4×10^{-13} ergs s^{-1} cm^{-2}, which would imply a dimming by a factor greater than 100. This is not compatible with the persistent nature of the IBIS source.
Source #1 (labelled as #2 in Landi et al. 2017) has 898 counts and only 75 above 3 keV. Source #2 has 174 counts, and 50 above 3 keV. Therefore, source #1 is much softer (it was also undetected above 3 keV in XRT) compared with #2. According to Landi et al. (2017), source #1 coincides with a *XMM–Newton* Slew source and with a *ROSAT* Bright object, and is identified as a star of type G, unlikely to emit at soft gamma-ray energies.
Chandra coordinates of source #1:
RA = 17:51:06.83
DEC = -32:18:27.92
error box = 3 arcsec
Chandra coordinates of source #2:
RA = 17:51:08.75
DEC = -32:21:22.45
error box = 2.5 arcsec
The spectra of the two sources are plotted in Fig. 10. Source #1 has a 0.3–10 flux of 4.7×10^{-12} ergs s^{-1} cm^{-2}, and a steep photon index $\Gamma = 2.9 \pm 0.1$. Source #2 has

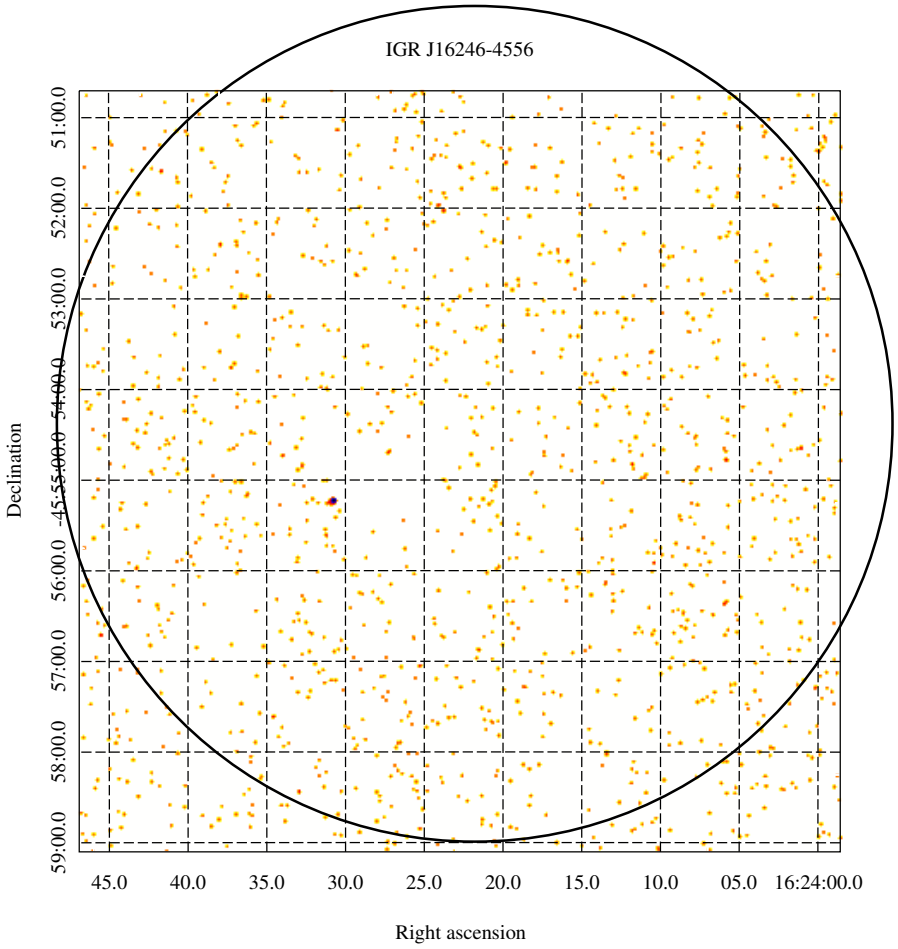

Figure 7: 3–10 keV *Chandra* image of the IGR J16246-4556 field. One source is detected.

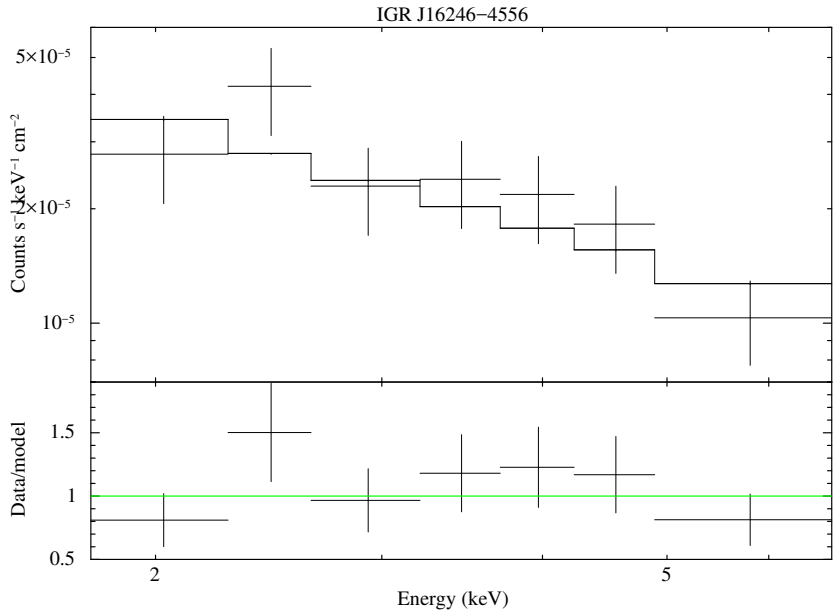

Figure 8: *Chandra* spectrum of IGR J16246-4556.

a 0.3–10 flux of 8.7×10^{-13} ergs s^{-1} cm^{-2}, and a photon index $\Gamma = 1.4 \pm 0.3$. This shows that the IBIS source is unlikely #1, which has an extrapolated 20–100 keV flux of 1×10^{-13} ergs s^{-1} cm^{-2}. Source #2 has an extrapolated 20–100 keV flux of 2×10^{-12} ergs s^{-1} cm^{-2}, still lower than the flux measured by IBIS (1.3×10^{-11} ergs s^{-1} cm^{-2}). Therefore, in this case we do not have a convincing association yet. We note however that source #2 is associated in SIMBAD with the dwarf nova OGLE BLG-DN-184 (U Geminorum-type). Dwarf novae are a type of cataclysmic variables consisting of a close binary system, in which one source is a white dwarf accreting from a normal stellar companion. OGLE BLG-DN-184 shows an outburst frequency of 3.17 yrs and a mean outburst duration of 13 days (Mróz et al., 2015). This may explain the different X-ray flux seen in the IBIS and *Chandra* epochs.

2.9 IGR J17096-2527

Detected as a persistent source in the 18-60 keV band.
Only a faint source is detected in *Chandra*, having 32 counts and only 10 above 3 keV. It is unlikely to be the counterpart of the bright, persistent IBIS source, given the low *Chandra* flux.

2.10 IGR J17118-3155

Detected in a 35.6 day outburst from MJD=52872.7.
Only a faint source is detected in *Chandra*, having 23 counts and only 10 above 3 keV.

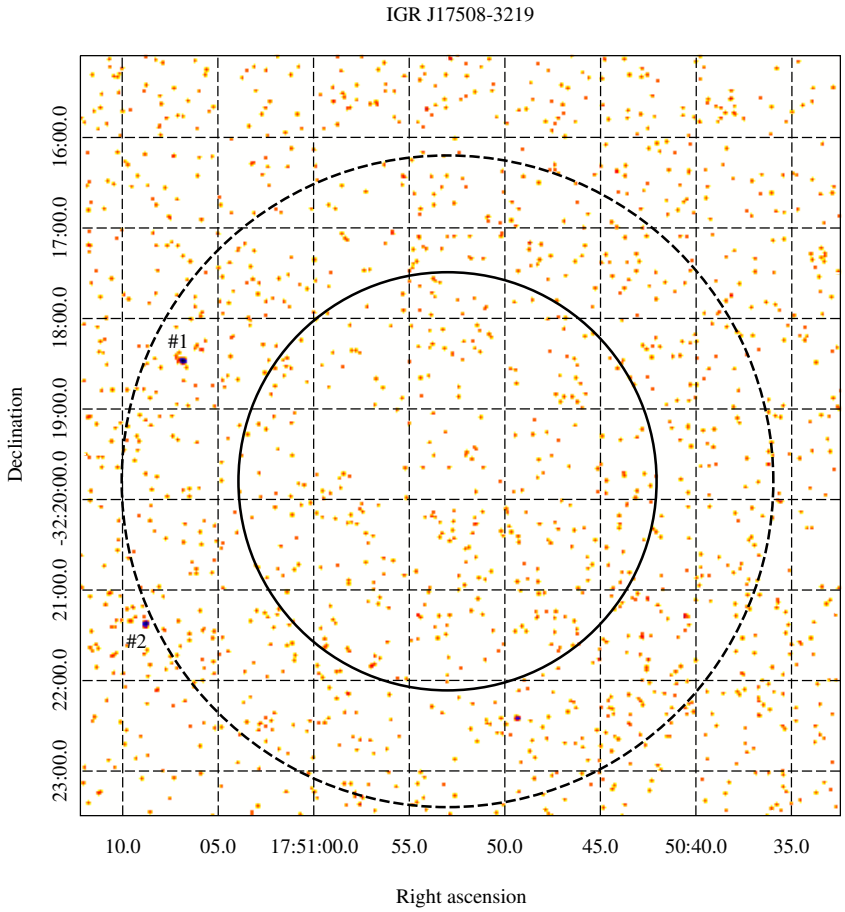

Figure 9: 3–10 keV *Chandra* image of the IGR J17508-3219 field. Two sources are detected. Source #1 is brighter and lies within the IBIS 99% error box (dashed circle). Nonetheless, source #2 is much harder and has a larger extrapolated 20-100 keV flux.

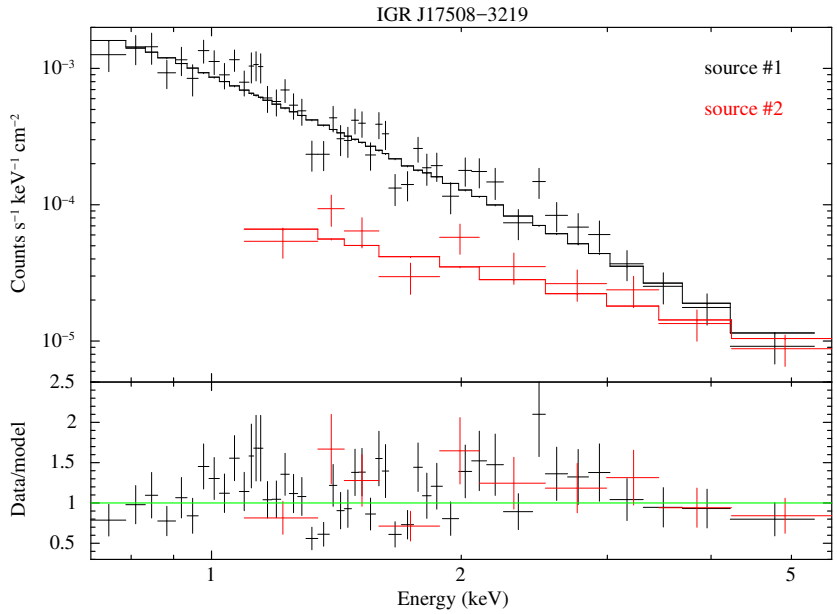

Figure 10: *Chandra* spectrum of source #1 and #2 detected in the *Chandra* image of IGR J17508-3219.

2.11 IGR J19294+1327

Detected as a persistent source in the 18-60 keV band.
A weak source is detected in *Chandra*, having 40 counts and 37 above 3 keV. If confirmed, this could be a hard source with $\Gamma = -1.5 \pm 0.8$ (possibly indicating heavy absorption) and a 0.3–10 keV flux of 8×10^{-13} ergs s^{-1} cm^{-2}. The image and spectrum are shown in Fig. 11 and 12.
Chandra coordinates:
RA = 19:29:30.10
DEC = +13:27:05.50
error box = 1.5 arcsec
Within the *Chandra* error circle we found the infrared source 2MASS J19293011+1327056. This source is also reported in WISE with colours W1-W2=0.279 and W2-W3=2.574, not typical of AGNs (Secrest et al., 2015) unless this is a Compton-thick source (Gandhi et al., 2015).

2.12 IGR J20310+3835

Detected as a persistent source in the 20-40 keV band.
One source is detected in *Chandra* (Fig. 13), with 294 counts (234 above 3 keV).
Chandra coordinates:
RA = 20:30:55.28
DEC = +38:33:46.65
error box = 2 arcsec
The spectrum is hard, with $\Gamma = -0.4 \pm 0.3$ (Fig. 14). The 0.3–10 keV flux is 3.8×10^{-12}.

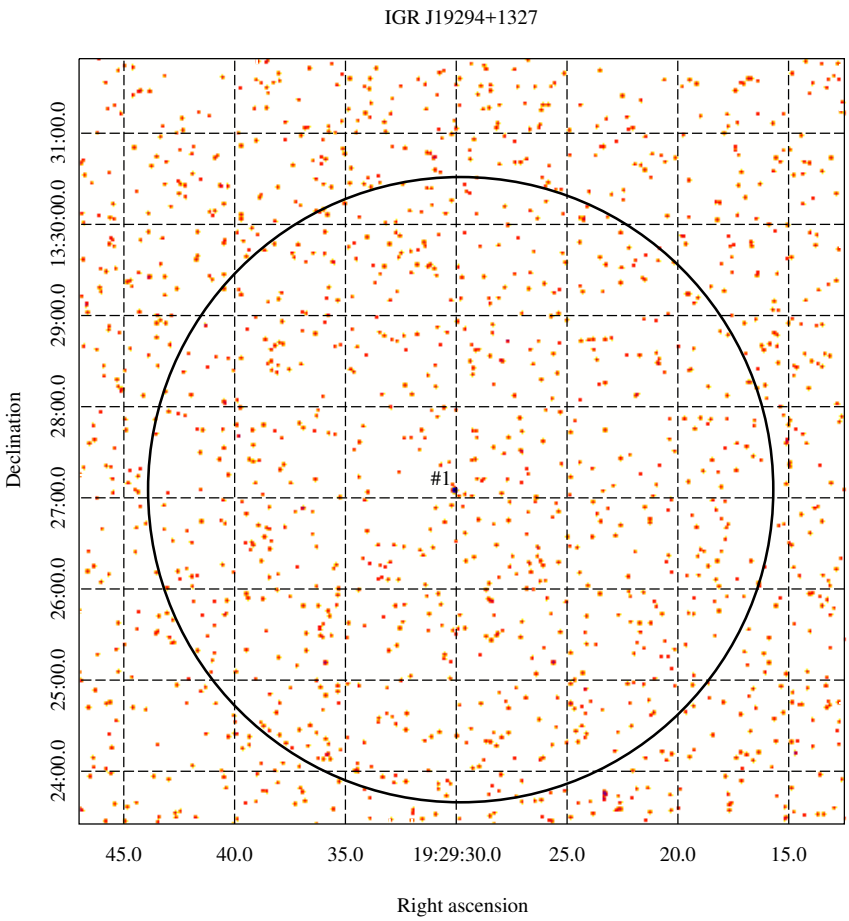

Figure 11: 3–10 keV *Chandra* image of the IGR J19294+1327 field. A weak source is detected.

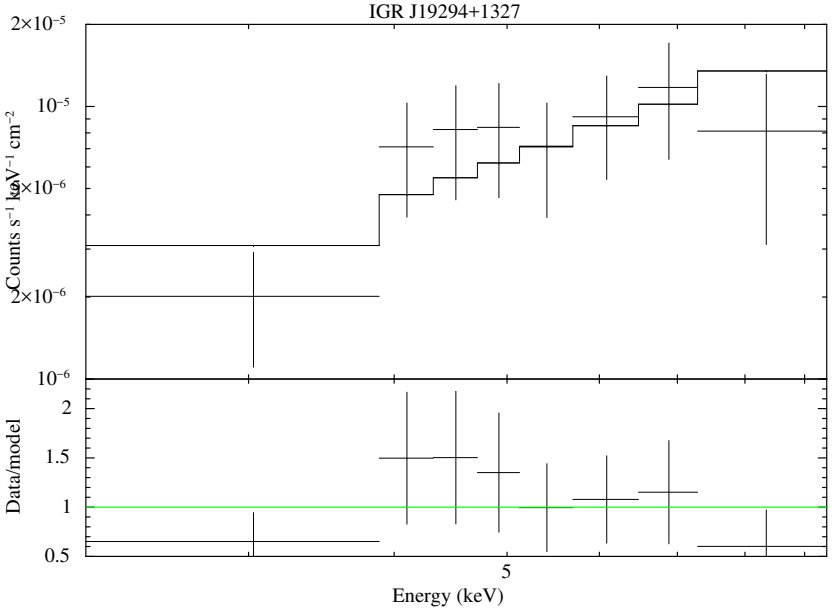

Figure 12: *Chandra* spectrum of the weak source in the *Chandra* image of IGR J19294+1327. The spectrum is binned for plotting purposes.

This source was also detected in XRT (Landi et al., 2017) and it is unclear at this stage whether it is a Galactic source or an AGN.

2.13 IGR J20413+3210

Detected in a 1.6 day outburst from MJD=54014.9.
No source is detected in *Chandra*.

References

Bird A. J., et al., 2016, ApJS, 223, 15

Evans I. N., et al., 2010, ApJS, 189, 37

Freeman P. E., Kashyap V., Rosner R., Lamb D. Q., 2002, ApJS, 138, 185

Gandhi P., Yamada S., Ricci C., Asmus D., Mushotzky R. F., Ueda Y., Terashima Y., La Parola V., 2015, MNRAS, 449, 1845

Landi R., et al., 2017, MNRAS, 470, 1107

Mróz P., et al., 2015, AcA, 65, 313

Secrest N. J., Dudik R. P., Dorland B. N., Zacharias N., Makarov V., Fey A., Frouard J., Finch C., 2015, ApJS, 221, 12

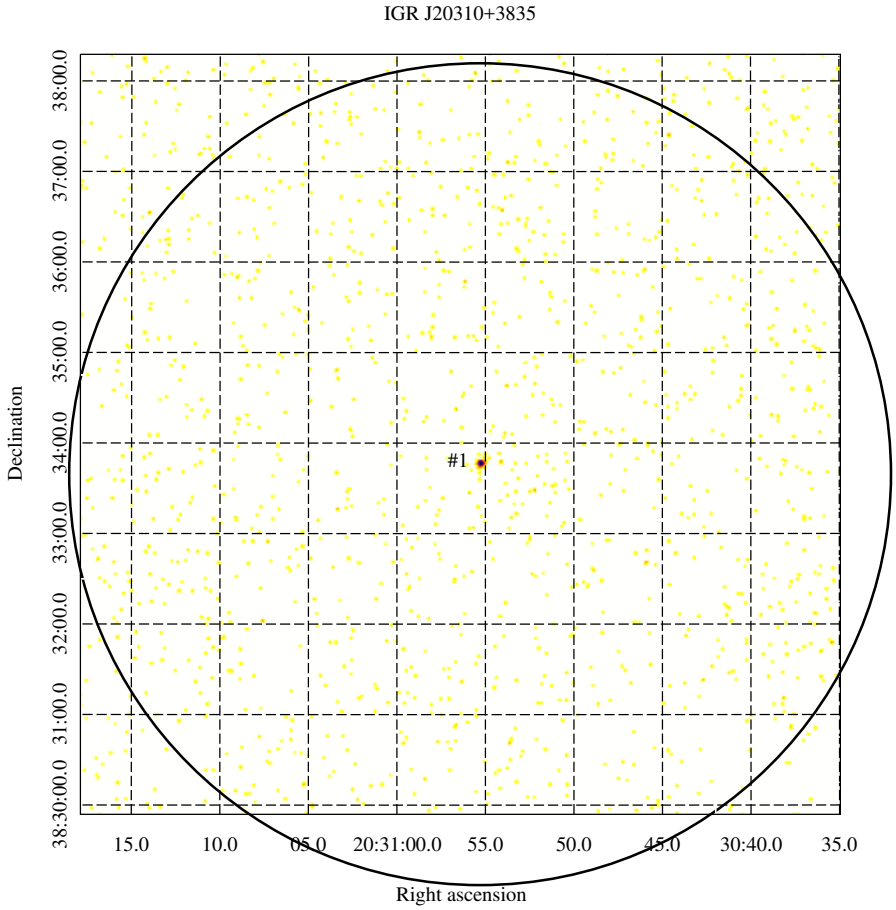

Figure 13: 3–10 keV *Chandra* image of the IGR J20310+3835. One source is detected.

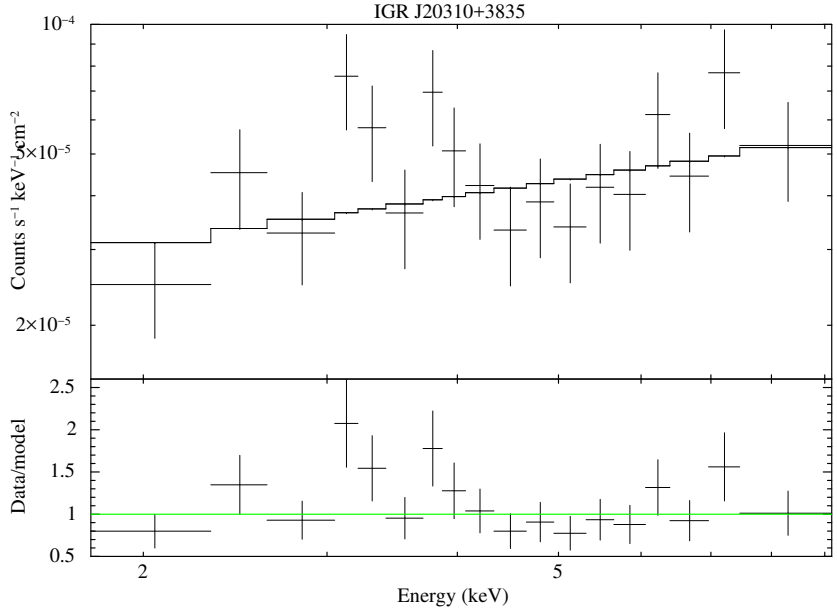

Figure 14: *Chandra* spectrum of IGR J20310+3835.

Staveley-Smith L., Kraan-Korteweg R. C., Schröder A. C., Henning P. A., Koribalski B. S., Stewart I. M., Heald G., 2016, AJ, 151, 52